

ResponsesReallocation of elemental content and macromolecule ~~of~~in the
coccolithophore *Emiliana huxleyi* to ~~reduced-phosphorus-availability and ocean~~
~~acidification depend on light intensity~~acclimate to climate change

Yong Zhang^{1,*}, Yong Zhang^{1,§}, Shuai Ma¹, Hanbing Chen², Jiabing Li¹, Zhengke
Li³, Kui Xu⁴, Ruiping Huang⁵, Hong Zhang¹, Yonghe Han¹, Jun Sun⁶

¹College of Environmental and Resource Sciences, College of Carbon Neutral
Modern Industry, Fujian Key Laboratory of Pollution Control and Resource
Recycling, Fujian Normal University, Fuzhou, China

²College of Life Science, Fujian Normal University, Fuzhou, China

³School of Food and Biological Engineering, Shanxi University of Science and
Technology, Xi'an, China

⁴Hubei Key Laboratory of Edible Wild Plants Conservation and Utilization, Hubei
Engineering Research Center of Special Wild Vegetables Breeding and
Comprehensive Utilization Technology, College of Life Sciences, Hubei Normal
University, Huangshi, China

⁵State Key Laboratory of Marine Environmental Science, College of Ocean and Earth
Sciences, Xiamen University, Xiamen, China

⁶Institute for Advanced Marine Research, China University of Geosciences,
Guangzhou, China

Running head: Physiology and biochemistry of *E. huxleyi*

*Correspondence: Yong Zhang (yongzhang@fjnu.edu.cn)

Keywords: Carbohydrate; CO₂; coccolithophore; elemental content; light intensity; phosphorus availability; protein.

§Email: qsx20211022@student.fjnu.edu.cn

51 Abstract

52 Global climate change leads to simultaneous changes in multiple environmental
53 drivers in the marine realm. Although physiological characterization of
54 coccolithophores have been studied under climate change, there is limited knowledge
55 on the biochemical responses of this biogeochemically important phytoplankton
56 group to changing multiple environmental drivers. Here we investigate the interactive
57 effects of reduced phosphorus availability (4 to 0.4 $\mu\text{mol L}^{-1}$), elevated $p\text{CO}_2$
58 concentrations (426 to 946 μatm) and increasing light intensity (40 to 300 $\mu\text{mol photons m}^{-2} \text{ s}^{-1}$) on elemental content and macromolecules of the cosmopolitan
60 coccolithophore *Emiliana huxleyi*. Reduced phosphorus availability reduces
61 particulate organic nitrogen and protein contents per cell under 40 $\mu\text{mol photons m}^{-2}$
62 s^{-1} low light intensity, but not under 300 $\mu\text{mol photons m}^{-2} \text{ s}^{-1}$ high light intensity.
63 Reduced phosphorus availability and ~~ocean acidification~~ elevated $p\text{CO}_2$
64 concentrations act synergistically to increase particulate organic carbon (POC) and
65 carbohydrate contents per cell under ~~high light intensity~~ 300 $\mu\text{mol photons m}^{-2} \text{ s}^{-1}$ but
66 not under ~~low light intensity~~ 40 $\mu\text{mol photons m}^{-2} \text{ s}^{-1}$. Reduced phosphorus
67 availability, ~~ocean acidification~~ elevated $p\text{CO}_2$ concentrations and increasing light
68 intensity act synergistically to increase the allocation of POC to carbohydrates. Under
69 ~~future ocean acidification~~ elevated $p\text{CO}_2$ concentrations and increasing light intensity,
70 enhanced carbon fixation could increase carbon storage in the phosphorus-limited
71 regions of the oceans where *E. huxleyi* dominates the phytoplankton assemblages. In
72 each light intensity, elemental carbon to phosphorus (C : P) and nitrogen to
73 phosphorus (N : P) ratios decrease with increasing growth rate. These results suggest
74 that coccolithophores could reallocate chemical elements and energy to synthesize
75 macromolecules efficiently, which allows them to regulate its elemental content and

growth rate to acclimate to changing environmental conditions.

1 Introduction

Continuous increase in atmospheric CO₂ level, as a consequence of anthropogenic activities, leads to global and ocean warming, which in turn shoals the ocean upper mixed layer (UML), hinders upward transport of nutrients from deeper ocean to the UML and increases light exposures to phytoplankton cells dwelling therein (Steinacher et al., 2010; Wang et al., 2015). The dissolution of CO₂ in the oceans is causing a significant chemical shift toward higher CO₂ and proton ([H⁺]) concentrations, a process defined as ocean acidification (OA) (Caldeira and Wickett, 2003). ~~These ocean changes expose phytoplankton cells within the UML to multiple drivers~~Environmental changes in the UML will expose phytoplankton cells to physiological stress, and understanding the effects of changing multiple environmental drivers on the physiology and biochemistry of marine phytoplankton is important for projections of changes in the biogeochemical roles of phytoplankton in the future ocean (Gao et al., 2019).

Coccolithophores take up carbon dioxide (CO₂) to produce particulate organic carbon (POC) via photosynthesis, and use bicarbonate (HCO₃⁻) and calcium (Ca²⁺) to synthesize calcium carbonate plates (coccoliths, PIC) and release CO₂ via calcification, and play a critical role in the marine carbon cycle (Rost and Riebesell, 2004). The cosmopolitan coccolithophore *Emiliania huxleyi* typically forms extensive blooms that are easily detected by satellite remote sensing due to high light scattering caused by coccoliths (Terrats et al., 2020; He et al., 2022). Within *E. huxleyi* blooms in polar and subpolar oceans, dissolved nitrate and phosphate concentrations in surface seawater could be as lower as 0.95 μmol L⁻¹ and 0.16 μmol L⁻¹, respectively

(Townsend et al., 1994), light intensity are higher than 300 $\mu\text{mol photons m}^{-2} \text{ s}^{-1}$ (Tyrrell and Merico, 2004), and the mean concentrations of seawater CO_2 increased by 21.0%–43.3% which weakens the oceanic CO_2 uptake from the atmosphere (Kondrik et al., 2018). *Emiliania huxleyi* is also the dominant phytoplankton species in the lower photic zone in the north-eastern Caribbean Sea (western Atlantic Ocean) (Jordan and Winter, 2000) and in the South Pacific Gyre where dissolved nitrate and phosphate concentration are about 1.0 $\mu\text{mol L}^{-1}$ and 0.2 $\mu\text{mol L}^{-1}$, respectively, and light intensity is lower than 20 $\mu\text{mol photons m}^{-2} \text{ s}^{-1}$ (Beaufort et al., 2008; Perrin et al., 2016). In the future ocean, numerous environmental factors will simultaneously change and the extent of these changes may increase (Gao et al., 2019). To explore how *E. huxleyi* acclimate to simultaneous changes in macronutrient concentration, light intensity and CO_2 level, it is interesting to investigate their physiological and biochemical processes, which can also help to project the effect of coccolithophores on ocean carbon cycle and ecological systems.

For more than a decade, research has shown that *E. huxleyi* cells developed several strategies to acclimate to reduced phosphorus availability, increasing light intensity and ocean acidification (Leonardos and Geider, 2005; McKew et al., 2015; Wang et al., 2022). Interactive effects of phosphorus availability and light intensity have shown that under phosphorus limitation condition, cells increased expression and the activity of alkaline phosphatase, and took up and used phosphorus efficiently under high light intensity, whereas they lowered the phosphorus uptake rate under low light intensity (Riegman et al., 2000; Perrin et al., 2016). In addition, the positive effect of reduced phosphorus availability on cellular POC and PIC contents of *E. huxleyi* was further enhanced by increasing light intensity due to high-light-induced increases in CO_2 and HCO_3^- uptake rates under low phosphate availability (Leonardos and Geider,

2005). The negative effect of reduced phosphorus availability on cellular particulate organic phosphorus (POP) content was partly compensated by increased PO_4^{3-} uptake rate under increasing light intensity (Perrin et al., 2016). On the other hand, several studies report that ocean acidification and reduced phosphorus availability acted synergistically to increase the cellular POC content, especially at high light intensity, and acted antagonistically to affect cellular PIC content of *E. huxleyi* (Leonardos and Geider, 2005; Matthiessen et al., 2012; Zhang et al., 2020). In addition, ocean acidification normally amplified the positive effect of increasing light intensity on cellular POC content (Rokitta and Rost, 2012; Heidenreich et al., 2019). Due to high proton concentration-induced reduction in HCO_3^- uptake rate, ocean acidification could weaken or counteract the positive effect of increasing light intensity on cellular PIC content (Rokitta and Rost, 2012; Kottmeier et al., 2016). Overall, while recent studies have focused on physiological performance of *E. huxleyi* and their effects on marine biogeochemical cycling of carbon, little information is available about the biochemical response of *E. huxleyi* to reduced phosphorus availability, increasing light intensity and ocean acidification.

The objective of this study is to investigate the combined effects of reduced phosphorus availability, increasing light intensity and ocean acidification on cellular elemental contents, the carbon (C) : nitrogen (N) : phosphorus (P) ratio and macromolecules of *E. huxleyi*, and to analyze the effects of macromolecules on elemental contents. Under reduced phosphorus availability, increasing light intensity and ocean acidification, we hypothesize that increased cellular POC content is more likely to be caused by increased carbohydrate content. In addition, we discuss the potential mechanisms for changing cellular PIC content in response to changed levels of phosphate, light, and CO_2 , which is important for projections of changes in

coccolithophore biogeochemistry and ecology in the future ocean.

2 Materials and Methods

2.1 Experimental setup

Emiliana huxleyi strain RCC1266 (morphotype A) was originally isolated from shelf waters around Ireland (49°30' N, 10°30' W) [in 2007](#) and obtained from the Roscoff algal culture collection ([Fig. S1](#)). *Emiliana huxleyi* was cultured under a 14 h : 10 h light : dark cycle (light period: 06:00 to 20:00 h) in a thermo-controlled incubator (MGC-400H, Shanghai Yiheng Scientific Instrument) at 20°C in semicontinuous cultures. The artificial seawater (ASW) media was prepared according to Berges et al. (2001) [with a salinity of 33 psu, a boron concentration of 372 \$\mu\text{mol L}^{-1}\$, and](#) with the addition of 2350 $\mu\text{mol L}^{-1}$ bicarbonate to achieve the total alkalinity (TA) of 2350 $\mu\text{mol L}^{-1}$, and enriched with 64 $\mu\text{mol L}^{-1}$ NO_3^- , f/8 concentrations for trace metals and vitamins (Guillard and Ryther, 1962). The experiment was conducted in two parts ([Fig. S24](#)). The first part (Part 1) was performed at 40 $\mu\text{mol photons m}^{-2} \text{s}^{-1}$ (low light intensity, LL) and the second one (Part 2) was at 300 $\mu\text{mol photons m}^{-2} \text{s}^{-1}$ (high light intensity, HL). The LL intensity used here corresponds to the lower end of the irradiance range of the UML, and the HL intensity represents to the irradiance in the surface ocean (Jin et al., 2016; Perrin et al., 2016). For each part of the experiment, dissolved inorganic phosphorus (DIP) concentration and ocean acidification were combined in a fully factorial design: high DIP concentration (4 $\mu\text{mol L}^{-1}$)+low CO_2 level (426 μatm , current CO_2 level) (HP+LC, treatment 1 in LL and treatment 5 in HL), high DIP concentration (4 $\mu\text{mol L}^{-1}$)+high CO_2 level (946 μatm , future CO_2 level) (HP+HC, treatment 2 in LL and treatment 6 in HL), low DIP concentration (0.43 $\mu\text{mol L}^{-1}$)+low CO_2 level (426 μatm) (LP+LC, treatment 3 in LL and treatment

176 7 in HL), and low DIP concentration ($0.43 \mu\text{mol L}^{-1}$)+high CO_2 level ($946 \mu\text{atm}$)
177 (LP+HC, treatment 4 in LL and treatment 8 in HL). High DIP concentration is replete
178 for physiological process of *E. huxleyi*, and ~~low DIP concentration corresponds to the~~
179 ~~upper end of the range of phosphate concentration in the coastal waters (Larsen et al.,~~
180 ~~2004)at the end of the incubation, low DIP concentration limits the growth of *E.*~~
181 ~~*huxleyi* (see below).~~ There were eight treatments totally and four biological replicates
182 for each treatment (Fig. S24). In all cases, cell densities were lower than 78,000 cells
183 mL^{-1} and the cells were acclimated to each treatment for at least 8 generations before
184 physiological and biochemical parameters were measured.

185 At LL intensity (Part 1), for the treatments of HP+LC and HP+HC, the ASW media
186 were enriched with $4 \mu\text{mol L}^{-1} \text{PO}_4^{3-}$ and aerated for 24 h at 20°C with filter-sterilized
187 (PTFE filter, $0.22 \mu\text{m}$ pore size, Nantong) air pumped from the room. The pH_{Total}
188 (total scale) values of the media under both HP+LC and HP+HC treatments were
189 about 8.04. The dry air was humidified with Milli-Q water prior to the aeration to
190 minimize evaporation. Under the HP+HC treatment, the pH_{Total} values of the media
191 were adjusted to 7.74 by stepwise additions of CO_2 -saturated seawater, ~~and the ratio~~
192 ~~was about 6.5 mL CO_2 -saturated seawater : 1000 mL ASW media. The CO_2 -saturated~~
193 ~~seawater was achieved by bubbling pure CO_2 -gas into 500 mL ASW media with a total~~
194 ~~alkalinity of $2350 \mu\text{mol L}^{-1}$ for 2 h.~~ For the treatments of LP+LC and LP+HC, the
195 ASW media were enriched with $0.4 \mu\text{mol L}^{-1} \text{PO}_4^{3-}$ and aerated for 24 h at 20°C with
196 filtered room air. Under the LP+HC treatment, the pH_{Total} values of the media were
197 also adjusted to 7.74 as described above. The HP+LC, HP+HC, LP+LC and LP+HC
198 seawater were then filtered ($0.22 \mu\text{m}$ pore size, Polycap 75 AS, Whatman) and
199 carefully pumped into autoclaved 50 mL (for TA measurements), 600 mL (for
200 pre-experimental cultures) and 2350 mL (for experimental cultures) polycarbonate

bottles (Nalgene) with no headspace to minimize gas exchange. The volumes of culture inoculum were calculated to match the volumes of media taken out from the bottles prior to inoculation. The cells were inoculated to achieve an initial density of 5000 cells ml⁻¹ in the HP+LC and HP+HC conditions, respectively, and cultured for 2 days, then diluted to the initial density again. These processes were performed three times in 600 mL bottles for pre-experimental cultures at 40 μmol photons m⁻² s⁻¹ (LL) of photosynthetically active radiation (PAR; measured using a LI-190SA quantum sensor, Beijing Ligaotai Technology Co. Ltd.). In the main experimental cultures ~~in the HP+LC and HP+HC conditions at LL intensity,~~ the cells were, respectively, transferred from 600 mL to 2350 mL bottles at the same time, and cultured for another 2 days (Fig. S2**4**b). Culture bottles were rotated 10 times until cells were mixed at 09:00 h, 13:00 h and 19:00 h. ~~Based on changes in cell densities during the incubations, we calculated that at LL intensity, cells were acclimated to HP+LC and HP+HC conditions for 10 generations.~~ In the second day of the main experimental cultures, subsamples were taken for measurements of cell densities, pH_{Total}, TA, cellular contents of total particulate carbon (TPC), particulate organic carbon (POC), nitrogen (PON) and phosphorus (POP), carbohydrate and protein. At the end of the cultures under the previous conditions, cell samples with an initial density of 5000 cells ml⁻¹ were transferred from HP+LC condition (treatment 1) to LP+LC condition (treatment 3), and from HP+HC condition (treatment 2) to LP+HC condition (treatment 4) at LL intensity. The cells were acclimated to LP+LC and LP+HC conditions for 8 generations before subsamples were taken for measurements, which allows cells to have enough time periods to change growth rate against the low DIP concentration.

At HL intensity (Part 2), samples grown under the HP+LC and HP+HC conditions

were transferred from 40 (LL) to 300 $\mu\text{mol photons m}^{-2} \text{ s}^{-1}$ (HL) of PAR with initial cell density of 5000 cells ml^{-1} . The cells were cultured under the HP+LC and HP+HC conditions for 2 days, respectively, and then diluted back to the initial cell density. These processes were performed three times in 600 mL bottles at HL intensity, and then the main experimental cultures were conducted in 2350 mL bottles. ~~The cells were, respectively, acclimated to HP+LC and HP+HC conditions for at least 8 generations at HL intensity.~~ On the second day of the incubation, subsamples were taken for measurements of the parameters. After that, cell samples with an initial density of 5000 cells ml^{-1} were transferred from HP+LC condition (treatment 5) to LP+LC condition (treatment 7), and from HP+HC condition (treatment 6) to LP+HC condition (treatment 8). At HL intensity, cell samples were acclimated for at least 8 generations in LP+LC and LP+HC conditions, respectively, before subsamples were taken for measurements.

2.2 Phosphate concentration and carbonate chemistry measurements

In the beginning and on the second day of the incubations, samples for determinations of phosphate concentration (20 mL), pH_{Total} value (20 mL) and total alkalinity (TA) (50 mL) were, respectively, filtered (PTFE filter, 0.22 μm pore size, Nantong) 7 h after the onset of the light period (at 13:00). Dissolved inorganic phosphorus (DIP) concentration was measured using a spectrophotometer (SP-722, Shanghai Spectrum Instruments) following the phosphomolybdate method (Hansen and Koroleff, 1999). The bottle for pH measurement was filled from bottom to top with overflow and closed without a headspace. The pH_{Total} value was measured immediately at 20°C using a pH meter which was corrected with a standard buffer of defined pH in seawater (Dickson, 1993). TA samples were treated with 10 μL saturated HgCl_2

solution and stored in the dark at 4.0°C, and TA was measured at 20°C by potentiometric titration (AS-ALK1+, Apollo SciTech) according to Dickson et al. (2007). Carbonate chemistry parameters were estimated from TA and pH_{Total} using the CO2SYS program of Pierrot et al. (2006) with carbonic acid constants, K_1 and K_2 , taken from Roy et al. (1993).

2.3 Cell density and elemental content measurements

Twenty milliliter samples to monitor the cell density were taken daily at 13:30 h, and fresh media with the same DIP concentration and carbonate chemistry as in the initial treatment conditions were added as top-up. Cell densities were determined using a MultisizerTM3 Coulter Counter (Beckman Coulter). Growth rates were calculated for each replicate according to the equation: $\mu = (\ln N_t - \ln N_0) / d$, where N_t and N_0 refer to the cell densities on the second day and in the beginning of the main experiment, respectively, and d was the growth period in days.

After mixing, samples for determinations of TPC (300 mL), POC and PON (300 mL), and POP (300 mL) were obtained by filtering onto GF/F filters (precombusted at 450°C for 6 h) at the same time (14:00 h) in each treatment. For POC and PON measurements, samples were fumed with HCl for 12 h to remove inorganic carbon. TPC, POC and PON samples were dried at 60°C for 12 h and analyzed using an Elementar CHNS analyzer (Vario EL cube, GmbH, Germany). Cellular particulate inorganic carbon (PIC) content was calculated as the difference between cellular TPC and POC contents (Fabry and Balch, 2010). To remove dissolved inorganic phosphorus from the GF/F filters, POP samples were rinsed three times with 0.17 mol L⁻¹ Na₂SO₄. After that, 2 mL 0.017 mol L⁻¹ MgSO₄ solution was added onto filters, and POP samples were dried at 90°C for 12 h, and then combusted at 500°C for 6 h to

remove POC and digested by 0.2 mol L⁻¹ HCl (Solórzano and Sharp, 1980). Phosphorus concentration was measured using a microplate reader (Thermo Fisher) following the ammonium molybdate method (Chen et al., 1956) using adenosine-5-triphosphate disodium trihydrate as a standard.

2.4 Protein and carbohydrate measurements

Samples for determinations of protein (600 mL) and carbohydrate (600 mL) were, respectively, filtered onto polycarbonate filters (0.6 µm pore size, Nuclepore, Whatman) and onto precombusted GF/F filters at 14:30 h. Protein samples were extracted by bead milling (FastPrep Lysing Matrix D) in 0.5 mL 1 × protein extraction buffer (lithium dodecyl sulfate, ethylene diamine tetraacetic acid, Tris, glycerol and 4-(2-aminoethyl) benzenesulfonyl fluoride hydrochloride). Bead milling was performed four times for 1 min at 6.5 ms⁻¹, and samples were placed on ice for 2 min between each round of bead milling to prevent degradation. The samples were then centrifuged at 10,000 × g for 5 min (Centrifuge 5418 R, Eppendorf, Germany), and extracted protein in the supernatant was quantified using the BCA assay with bovine gamma globulin as a standard using a microplate reader (Ni et al., 2016). Carbohydrate (or polysaccharide) samples were hydrolyzed with 12.00 mol L⁻¹ H₂SO₄ in the dark for 1 h and diluted by Milli-Q water to a final H₂SO₄ concentration of 1.20 mol L⁻¹. Then, samples were sonicated for 5 min, vortexed for 30 s, and boiled at 90°C for 3 h (Pakulski and Benner, 1992). The extracted carbohydrate was determined by phenol sulfuric reaction with D-glucose as standard (Masuko et al., 2005).

2.5 Data analysis

The percentages of carbon (C : carbohydrate is 40% and C : protein is 53%) and nitrogen (N : protein is 16%) contributed by carbohydrate and protein were calculated from the elemental composition of biochemical classes compiled by Geider and LaRoche (2002). A three-way ANOVA was used to determine the main effects of DIP concentration, light intensity and CO₂ level, and their interactions on each variable. A Tukey post hoc test was performed to identify significant differences between two DIP concentrations, two light intensities and two CO₂ levels. A Shapiro–Wilk test was conducted to analyze the normality of residuals and a Levene test was conducted graphically to test for homogeneity of variances. The significant difference between treatments was set at $p < 0.05$. All data analyses were conducted using the statistical software *R* with the packages *carData*, *lattice* and *nlme* (*R* version 3.5.0).

3 Results

3.1 Dissolved inorganic phosphorus concentration and carbonate chemistry parameters

During the incubations, organismal activity significantly reduces dissolved inorganic phosphorus (DIP) concentrations (Table 1). Under high phosphorus (HP) treatment, DIP concentrations decrease by 20.32% in low light (LL) and low CO₂ (LC), by 22.32% in LL and high CO₂ (HC), by 27.66% in high light (HL) and LC, and by 31.58% in HL and HC. Under low phosphorus (LP) treatment, DIP concentrations decrease from 0.43 $\mu\text{mol L}^{-1}$ at the beginning of the experiment to be lower than 0.04 $\mu\text{mol L}^{-1}$ (the detection limit) at the end of the incubation in LL and LC conditions, in LL and HC conditions, in HL and LC conditions, and in HL and HC conditions.

During the incubations, at LL intensity, pH_T values increase by, on average, 0.02 in HP+LC, by 0.03 in HP+HC, by 0.09 in LP+LC, and by 0.10 in LP+HC conditions

(Table 1). At HL intensity, pH_T values increase by 0.05 in HP+LC, by 0.06 in HP+HC, by 0.12 in LP+LC, and by 0.09 in LP+HC conditions. Correspondingly, at LL intensity, seawater CO_2 concentrations decrease by 5.53% in HP+LC, by 6.89% in HP+HC, by 22.76% in LP+LC, and by 22.77% in LP+HC. At HL intensity, seawater CO_2 concentrations decrease by 16.18% in HP+LC, by 16.41% in HP+HC, by 28.92% in LP+LC, and by 22.30% in LP+HC. Overall, organismal activity has larger effects on carbonate chemistry under the LP treatment than under the HP treatment.

3.2 Growth rate

The effect of increasing light intensity on growth rate is positive which can be seen by comparing growth rate in the HL regimes with their paired LL regimes (Fig. 1a,b; Table 2), though the extent of increase in growth rate depends on CO_2 levels and phosphate availability. Compared to LL intensity, growth rates at HL intensity increased by 48.48% in HP+LC, by 50.87% in HP+HC, by 60.86% in LP+LC, and by 60.80% in LP+HC (Tukey post hoc test, all values of $p < 0.01$). The effect of increasing CO_2 levels on growth rate depends on light intensity and phosphate availability (Fig. 1a,b). Compared to LC level, growth rates in HC level decreased by 3.08% in LL and HP condition ($p = 0.48$), by 16.13% in LL and LP condition ($p < 0.01$), by 1.50% in HL and HP condition ($p = 0.68$), and by 16.27% in HL and LP condition ($p < 0.01$). The effect of reduced phosphorus availability on growth rate is negative and the extent of reduction in growth rate depends on light intensity and CO_2 levels (Fig. 1a,b). Compared to HP availability, growth rates in LP availability decreased by 8.46% in LL and LC condition ($p < 0.01$), by 20.81% in LL and HC condition ($p < 0.01$), ~~by 0.76% in HL and LC condition ($p = 0.99$)~~, and by 15.63% in HL and HC condition ($p < 0.01$), and did not change significantly in HL and LC

condition ($p = 0.99$). These results show that high CO₂ levels and low phosphorus availability acted synergistically to reduce growth rate of *E. huxleyi*, and increasing light intensity could partly counteract this response (Table S1).

3.3 Cellular POC, PON, POP and PIC contents

The effect of increasing light intensity on cellular POC content is positive, which was observed by comparing POC content in all the HL regimes with their paired LL regimes (Fig. 1be,d). The extent of increase in POC content depends on CO₂ levels and phosphate availability. Compared to LL intensity, cellular POC contents at HL intensity increased by 27.15% in HP+LC, by 26.51% in HP+HC, by 43.24% in LP+LC, and by 58.13% in LP+HC conditions (Tukey post hoc test, all values of $p < 0.01$). The effect of increasing CO₂ levels on POC content is light and phosphate dependent and can be seen by comparing POC content in the HC regimes with their paired LC regimes (Fig. 1be,d). At LL intensity, cellular POC contents are not significantly different between HP+LC, HP+HC, LP+LC and LP+HC conditions (all values of $p > 0.1$). At HL intensity, compared to LC level, cellular POC contents in HC level increased by 5.12% in HP condition ($p = 0.74$), and by 8.28% in LP condition ($p = 0.07$). The effect of phosphate reduction on POC content is light and CO₂ dependent, which can be seen by comparing POC content in the LP regimes with those in their paired HP regimes (Fig. 1be,d). At LL intensity, cellular POC contents did not significantly differ between LP and HP availability. At HL intensity, compared to HP availability, cellular POC contents in LP availability increased by 11.80% in LC condition ($p = 0.02$), and by 15.28% in HC condition ($p < 0.01$). These results show that ocean acidification and reduced phosphorus availability acted synergistically to increase POC contents in HL condition but not in LL condition

(Table S1).

The effect of increasing light intensity on cellular PON content depends on CO₂ levels and phosphate availability (Fig. 1~~ce,f~~). Compared to LL intensity, cellular PON contents at HL intensity increased by 12.03% in HP+LC condition ($p = 0.27$), by 19.54% in HP+HC condition ($p < 0.01$), by 22.68% in LP+LC condition ($p < 0.01$), and by 30.90% in LP+HC condition ($p < 0.01$). The effect of increasing CO₂ levels on PON content is light and phosphate dependent, which can be seen by comparing POC content in the HC regimes with their paired LC regimes (Fig. 1~~ce,f~~). Compared to LC level, cellular PON contents in HC level did not change significantly in LL and HP condition, in LL and LP condition, in HL and LP condition, and increased by 14.68% in HL and HP condition ($p = 0.02$). The effect of phosphate reduction on PON content is CO₂ and light dependent, which can be seen by comparing PON content in the LP regimes with those in their paired HP regimes (Fig. 1~~ce,f~~). Compared to HP availability, cellular PON contents in LP availability decreased by 16.59% in LL and LC condition ($p = 0.01$), by 24.03% in LL and HC condition ($p < 0.01$), by 8.35% in HL and LC condition ($p = 0.43$), and by 17.32% in HL and HC condition ($p < 0.01$). These results show that increasing light intensity compensated for the negative effect of phosphate reduction on PON content (Table S1).

The effect of increasing light intensity on POP content is positive and can be seen by comparing POP content in the HL regimes with their paired LL regimes, though the extent of increase in POP content depends on CO₂ levels and phosphate availability (Fig. 1~~de,h~~). Compared to LL intensity, cellular POP contents at HL intensity increased by 35.79% in HP+LC, by 41.70% in HP+HC, by 57.22% in LP+LC, and by 56.44% in LP+HC conditions (Tukey post hoc test, all values of $p < 0.01$). Ocean acidification did not change the POP contents significantly ~~in LL and~~

~~HP condition, in LL and LP condition, in HL and HP condition, and in HL and LP~~
~~condition under all treatments used here~~ (all values of $p > 0.53$) (Fig. 1~~dg,h~~). Reduced
phosphorus availability significantly decreased the POP contents, which can be seen
by comparing POP content in the LP regimes with their paired HP regimes, though
the extent of reduction in POP content depends on light intensity and CO₂ levels (Fig.
1~~dg,h~~). Compared to HP availability, cellular POP contents in LP availability
decreased by 52.96% in LL and LC condition, by 54.03% in LL and HC condition, by
46.11% in HL and LC condition, and by 49.51% in HL and HC condition (all values
of $p < 0.01$). These results show that reduced phosphorus availability had a larger
effect on POP content than that of ocean acidification and increasing light intensity
(Table S1).

The effect of increasing light intensity on PIC content is positive, which can be
seen by comparing PIC content in the HL regimes with their paired LL regimes,
though the extent of increase in PIC content depends on CO₂ levels and phosphorus
availability (Fig. 1~~ei,j~~). Compared to LL intensity, cellular PIC contents at HL
intensity increased by 77.87% in HP+LC, by 70.28% in HP+HC, by 98.31% in
LP+LC, and by 90.68% in LP+HC conditions (Tukey post hoc test, all values of $p <$
0.01). The effect of increasing CO₂ levels on PIC content is negative and can be seen
by comparing PIC content in the HC regimes with those in their paired LC regimes
(Fig. 1~~ei,j~~). The extent of reduction in PIC content depends on light intensity and
phosphorus availability. Compared to LC level, cellular PIC contents under ocean
acidification decreased by 31.43% in LL and HP condition ($p = 0.09$), by 16.00% in
LL and LP condition ($p = 0.67$), by 35.02% in HL and HP condition ($p < 0.01$), and
by 21.12% in HL and LP condition ($p < 0.01$). The effect of phosphate reduction on
PIC content is positive which can be seen by comparing PIC content in the LP

regimes with their paired HP regimes, though the extent of increase in PIC content depends on light intensity and CO₂ levels (Fig. 1e,j). Compared to HP availability, cellular PIC contents in LP availability increased by 16.00% in LL and LC condition ($p = 0.83$), by 41.26% in LL and HC condition ($p = 0.16$), by 29.98% in HL and LC condition ($p < 0.01$), and by 60.44% in HL and HC condition ($p < 0.01$). These results show that high light intensity and low phosphorus availability acted synergistically to increase PIC content, which counteracts the negative effect of ocean acidification on PIC content (Table S1).

3.4 Carbohydrate and protein contents

The effect of increasing light intensity on carbohydrate content is positive and can be seen by comparing carbohydrate content in the HL regimes with their paired LL regimes, though the extent of increase in carbohydrate depends on CO₂ levels and phosphorus availability (Fig. 2a,b). Compared to LL intensity, cellular carbohydrate contents at HL intensity increased by 148.81% in HP+LC condition, by 139.42% in HP+HC condition, by 179.12% in LP+LC condition, and by 204.42% in LP+HC condition (all values of $p < 0.01$). The effect of increasing CO₂ levels on carbohydrate content is light and phosphate dependent which can be seen by comparing carbohydrate content in the HC regimes with their paired LC regimes (Fig. 2a,b). Compared to LC level, cellular carbohydrate contents under ocean acidification increased by 26.55% in LL and HP condition ($p = 0.58$), by 8.91% in LL and LP condition ($p = 0.99$), by 21.32% in HL and HP condition ($p = 0.02$), and by 18.45% in HL and LP condition ($p < 0.01$). The effect of phosphate reduction on carbohydrate content is light and CO₂ dependent and can be seen by comparing carbohydrate content in the LP regimes with their paired HP regimes (Fig. 2a,b). Compared to HP

availability, cellular carbohydrate contents in LP availability did not change significantly in LL and LC condition, in LL and HC condition (both $p > 0.65$) and increased by 40.13% in HL and LC condition ($p < 0.01$), and by 36.00% in HL and HC condition ($p < 0.01$). These results show that increasing light intensity dominantly increased carbohydrate content, and ocean acidification and reduced phosphorus availability acted synergistically to increase carbohydrate contents under high light intensity (Table S1).

The effect of increasing light intensity on cellular protein content is positive, which can be seen by comparing protein content in the HL regimes with their paired LL regimes, though the extent of increase in protein content depends on CO₂ level and phosphorus availability (Fig. 2b,e,d). Compared to LL intensity, cellular protein contents at HL intensity increased by 24.76% in HP+LC condition, by 30.43% in HP+HC condition, by 68.09% in LP+LC condition, and by 65.39% in LP+HC condition (all values of $p < 0.01$). The effect of increasing CO₂ levels on protein content can be seen by comparing protein content in the HC regimes with their paired LC regimes (Fig. 2b,e,d). Compared to LC level, cellular protein contents under ocean acidification did not change significantly in LL and HP condition, in LL and LP condition, in HL and HP condition, and in HL and LP condition (all values of $p > 0.09$). The effect of phosphate reduction on protein content is light and CO₂ dependent, which can be seen by comparing protein content in the LP regimes with their paired HP regimes (Fig. 2b,e,d). Compared to HP availability, cellular protein content in LP availability decreased by 27.88% in LL and LC condition, by 28.80% in LL and HC condition (both $p < 0.01$) and did not change significantly in HL and LC condition, and in HL and HC condition (both $p > 0.11$). These results show that high light intensity counteracted the negative effect of low phosphorus availability on

protein content, and ocean acidification had less effect on protein content [\(Table S1\)](#).

3.5 Percentage of POC allocated to carbohydrate (carbohydrate-C : POC) and protein (protein-C : POC)

Increasing light intensity increased the percentage of POC allocated to carbohydrate (carbohydrate-C : POC), which can be seen by comparing carbohydrate-C : POC in the HL regimes with their paired LL regimes, though the extent of increase in carbohydrate-C : POC depends on CO₂ levels and phosphorus availability (Fig. 2ce,f). Compared to LL intensity, carbohydrate-C : POC at HL intensity increased by 95.60% in HP+LC condition, by 97.69% in HP+HC condition, by 95.05% in LP+LC condition, and by 83.37% in LP+HC condition (all values of $p < 0.01$). The effect of increasing CO₂ levels on carbohydrate-C : POC is light and phosphate dependent, and can be seen by comparing carbohydrate-C : POC in the HC regimes with their paired LC regimes (Fig. 2ce,f). Compared to LC level, carbohydrate-C : POC under ocean acidification increased by 20.12% in LL and HP condition, by 11.42% in LL and LP condition, by 20.36% in HL and HP condition, and by 4.40% in HL and LP condition (all values of $p > 0.08$). The effect of phosphate reduction on carbohydrate-C : POC is light and CO₂ dependent, which can be seen by comparing carbohydrate-C : POC in the LP regimes with those in their paired HP regimes (Fig. 2ce,f). Compared to HP availability, carbohydrate-C : POC in LP availability increased by 25.61% in LL and LC condition ($p = 0.16$), by 17.37% in LL and HC condition ($p = 0.47$), by 25.81% in HL and LC condition ($p < 0.01$), and by 8.11% in HL and HC condition ($p < 0.05$). These results show that increasing light intensity, ocean acidification and reduced phosphorus availability acted synergistically to increase the percentage of POC allocated to carbohydrate [\(Table S1\)](#).

Increasing light intensity did not significantly change the percentage of POC allocated to protein (protein-C : POC) ~~in HP+LC, HP+HC, LP+LC and LP+HC conditions~~under the phosphorus availability and CO₂ levels used here (Fig. 2d,g,h). Ocean acidification did not significantly affect the protein-C : POC in LL and HP, in LL and LP, in HL and HP, and in HL and LP conditions. The effect of phosphate reduction on protein-C : POC is light and CO₂ dependent, which can be seen by comparing the protein-C : POC in the LP regimes with their paired HP regimes (Fig. 2d,g,h). Compared to HP availability, protein-C : POC in LP availability decreased by 27.39% in LL and LC condition ($p < 0.01$), by 23.05% in LL and HC condition ($p < 0.01$), by 12.81% in HL and LC condition ($p = 0.09$), and by 21.77% in HL and HC condition ($p < 0.01$). These results show that reduced phosphorus availability dominantly reduced the protein-C : POC, and increasing light intensity and ocean acidification had less effects on protein-C : POC (Table S1). On the other hand, increasing light intensity, reduced phosphorus availability and ocean acidification did not significantly change the percentage of PON allocated to protein (protein-N : PON) (Fig. 2e).

3.6 Elemental stoichiometry and protein content as a function of growth rate

Reduced phosphorus availability increased the POC : PON ratio, and the extent of the increase was larger under HL than LL intensity (Fig. S5a). At LL and HL intensities, both POC : POP ratio and PON : POP ratio were linearly and negatively correlated with growth rates (Fig. 3a,b). In LL and HL conditions, POC : POP ratio decreased linearly with increasing growth rate ($R^2 = 0.71$, $F = 32.08$, $p < 0.01$ in LL condition; $R^2 = 0.53$, $F = 14.63$, $p < 0.01$ in HL condition). Similarly, in LL and HL conditions, PON : POP ratio decreased linearly with increasing growth rate ($R^2 = 0.69$, $F = 29.23$,

$p < 0.01$ in LL condition; $R^2 = 0.50$, $F = 13.31$, $p < 0.01$ in HL condition). In all treatments, protein content increased linearly with increasing growth rate ($R^2 = 0.76$, $F = 151.14$, $p < 0.01$) (Fig. 3c), and POC content increased linearly with increasing carbohydrate content ($R^2 = 0.94$, $F = 435.10$, $p < 0.01$) (Fig. 3d).

4 Discussion

Coccolithophores ~~make an important contribution to marine biological carbon pump~~ play a complex role in the marine carbon cycle through production and export of organic carbon to depth but also through the carbonate counter pump, and their responses to global climate change could have significant consequences for marine carbon cycling (Riebesell et al., 2017). The bloom-forming coccolithophore *E. huxleyi*, dominating the assemblages in seawater under limited phosphorus condition, is likely to be exposed to increasing light intensity and ocean acidification in the future ocean (Kubryakova et al., 2021). In this study, we observed that increasing light intensity compensates for the negative effects of low phosphorus availability on cellular protein and nitrogen contents (Figs. 1 and 2). Reduced phosphorus availability, increasing light intensity and ocean acidification act synergistically to increase cellular contents of carbohydrate and POC, and the allocation of POC to carbohydrate. These ~~regulation mechanisms~~ changes in *E. huxleyi* could provide vital information for evaluating carbon cycle in marine ecosystems under global change.

Ribonucleic acid (RNA) is the main phosphorus-containing macromolecule within the cell (Geider and La Roche, 2002). Therefore, the reduced phosphorus availability dominantly reduces the RNA content (Fig. S65), which contributes to low POP contents (McKew et al., 2015) (Fig. 1d,g,h). In eukaryotic cells, ribosomal RNA (rRNA) constitutes about 80% of the total RNA and is mainly used to create ribosome

(Dyhrman, 2016). Thus, reduced RNA contents decrease the numbers of ribosome, which has a potential to decrease protein synthesis (Dyhrman, 2016; Rokitta et al., 2016). In addition, the separation of the regression line between POC : POP ratio (or PON : POP ratio) and growth rate under low and high light intensities suggests different POP storage contents in *E. huxleyi* among different light intensities (Perrin et al., 2016). On the other hand, low light intensity down-regulates the expression of genes related to nitrate reductase and nitrite reductase, and then reduces the nitrate uptake and assimilation efficiency of *E. huxleyi* and other phytoplankton species (Perrin et al., 2016; Lu et al., 2018), which exacerbates the negative effect of low phosphorus availability on protein synthesis and PON contents (Figs. 1~~ce~~ and 2~~be~~). Besides that, low light intensity significantly reduces the rates of RNA synthesis, carbohydrate synthesis and cell division (Zhang et al., 2021), which adds to the negative effect of low phosphorus availability on growth rate of *E. huxleyi* (Fig. 1a). Under high light intensity and low CO₂ level, reduced phosphorus availability did not change growth rate and protein content (Figs. 1~~ab~~ and 2~~bd~~), which suggests that *E. huxleyi* might compensate for low phosphate-induced decreases in ribosome content by increasing protein synthesis efficiency under increasing light intensity (Reith and Cattolico, 1985). Under high light intensity and ocean acidification, reduced phosphorus availability did not significantly change cellular protein content while reduced growth rate, which might indicate the lowered protein synthesis efficiency (McKew et al., 2015).

Several studies report that reduced phosphorus availability (0.4–0.5 $\mu\text{mol L}^{-1}$) did not change growth rates significantly during the short-time (2 or 3 days) incubations under low CO₂ level and high light intensity (Rokitta et al., 2016; Zhang et al., 2020; Wang et al., 2022) ~~(Fig. S6)~~. The reasons could be that *E. huxleyi* cells developed

high affinity for phosphate and increased the uptake rate of phosphate (Wang et al., 2022) and could replace the phospholipid membrane with non-phosphorus membrane during the short-time incubation of phosphorus limitation (Shemi et al., 2016). Our data showed that reduced phosphorus availability and ocean acidification acted synergistically to reduce growth rate under both low and high light intensities (Fig. 1a,b). One of the reasons could be that low pH value under ocean acidification up regulates the expressions of a series of genes involved in ribosome metabolism, such as genes of large subunit ribosomal protein L3, L38E, L30E (*RP-L3*, *RP-L38E*, *RP-L30E*), and small subunit ribosomal protein S3E, S5E, SAE (*PR-S3E*, *PR-S5E*, *RP-SAE*) in *E. huxleyi* (Wilson and Doudna Cate, 2012) (Fig. S7). Under ocean acidification, up regulation of expression of these genes has the potential to drive cells to allocate more phosphorus to synthesize ribosome, and to reduce the allocation of phosphorus to DNA replication (Rokitta et al., 2011), which exacerbates the limitation of reduced phosphorus availability on the rate of cell division in *E. huxleyi* (Rouco et al., 2013). Under phosphorus-replete condition, more phosphorus is reallocated to ribosome metabolism under ocean acidification which could facilitate nitrogen assimilation (Fig. 2b,d). Overall, under high light intensity, ocean acidification is likely to facilitate *E. huxleyi* cells to increase nitrogen content in phosphorus-replete condition and to reduce growth rate in phosphorus-limitation.

In this study, we found that low light intensity dominantly limits carbon assimilation of *E. huxleyi* and reduces the effects of phosphate availability and ocean acidification on cellular carbohydrate and POC contents (Figs. 1b,e and 2a). However, under high light intensity, *E. huxleyi* had high carbohydrate and POC contents while low growth rate under reduced phosphorus availability and ocean acidification (Figs. 1a,b,b,d and 2a,b), which suggests that carbon assimilation rate did not change

significantly while cell division rate decreased (Matthiessen et al., 2012; Perrin et al., 2016). Furthermore, carbohydrate is a carbon- and energy-storing macromolecule, and protein is related to growth rate (Geider and La Roche, 2002). Under high light intensity, reduced phosphorus availability and ocean acidification, *E. huxleyi* cells could synthesize more carbohydrate to store carbon and energy but didn't increase protein content, which contributes to the large percentage of POC allocated to carbohydrate (Fig. 2cf).

The physiological reasons for reduced calcification rate under ocean acidification could be due to high proton concentration-induced reduction in HCO_3^- uptake rate (Meyer and Riebesell, 2015; Kottmeier et al., 2016). The molecular mechanisms for low PIC content under ocean acidification may be due to down-regulation of a series of genes potentially involved in ion transport and pH regulation, such as genes of calcium/proton exchanger (*CAX3*), sodium/proton exchanger (*NhaA2*) and membrane-associated proton pump (*PATP*) (Mackinder et al., 2011; Lohbeck et al., 2014). On the other hand, increasing light intensity up-regulates a series of genes related to ion transport, such as gene of *CAX3*, gene of $\text{Cl}^-/\text{HCO}_3^-$ exchanger and genes of various subunits of a vacuolar H^+ -ATPase (*V-ATPase*) and so on (Rokitta et al., 2011). Up-regulation of these genes in high light intensity has the potential to facilitate cells to take up HCO_3^- and Ca^{2+} , and to pump proton outside the cells, and then leads to large PIC content of *E. huxleyi* (Kottmeier et al., 2016). Our data suggest that increasing light intensity counteracts the negative effect of ocean acidification on cellular PIC content of *E. huxleyi* (Fig. 1ei-j). These results are consistent with the findings of Feng et al. (2020) who reported that combinations of increasing light intensity and ocean acidification increase the expression of genes involved in calcium-binding proteins (*CAM* and *GPA*), which has the potential to increase

calcium influx into cells and then compensate for the effect of reduced HCO_3^- uptake rate on calcification. It is also suggested that increasing light intensity could cause cells to remove H^+ faster which neutralizes the effect of high proton concentration on calcification (Jin et al., 2017). On the other hand, reduced phosphorus availability extends the G1 phase of cell cycle where calcification occurs, which prolongs the calcification time and then increases cellular PIC content (Müller et al., 2008). In addition, reduced phosphorus availability up-regulates expressions of genes of Ca^{2+} uptake, proton removal and carbonic anhydrase, and then increases coccolith production (Wang et al., 2022), which contribute to a larger PIC content and counteract the negative effect of ocean acidification on PIC contents (Borchard et al., 2011) (Fig. 1e+j). Furthermore, one of the reasons for larger PIC contents under reduced phosphorus availability and increasing light intensity conditions are likely due to larger and more numerous coccoliths (Gibbs et al., 2013; Perrin et al., 2016). Overall, responses of calcification of *E. huxleyi* to ocean climate change are complex than previously thought (Meyer and Riebesell, 2015), and it is worth exploring the underlying mechanisms of calcification under changing multiple environmental drivers (Mackinder et al., 2011; Feng et al., 2020).

Cellular POP content of *E. huxleyi* generally decreased, and POC : POP ratio and PON : POP ratio increased with reducing phosphorus availability (Leonardo and Geider, 2005; McKew et al., 2015). The negative correlations between growth rate and POC : POP ratio or PON : POP ratio under each light intensity are consistent with the growth rate hypothesis (Fig. 3), which proposes that growth rate increases with increasing RNA : protein ratio. Phosphorus in RNA accounts for a high percentage of total POP, whereas nitrogen in protein is the main form of PON (Zhang et al., 2021), and the growth rate hypothesis suggests that growth rate could increase with

decreasing POC : POP ratio or PON : POP ratio (Sterner and Elser, 2002). Our results suggest that *E. huxleyi* could reallocate chemical elements and energy to synthesize carbohydrate, protein and RNA efficiently, and then regulate its elemental stoichiometry and growth rate to acclimate to reduced phosphorus availability, ocean acidification and increasing light intensity (Moreno and Martiny, 2018).

In the future ocean, large carbohydrate and POC contents, POC : PON ratio, and POC : POP ratio of coccolithophores indicate increases in carbon export to the deep ocean that may affect the efficiency of the biological carbon pump and the marine biogeochemical cycle of carbon (Meyer and Riebesell, 2015). In addition, increased cellular PIC content under phosphorus limitation condition may have the potential to weaken CO₂ uptake of the oceans in phosphorus-limited marine environments. In summary, responses of coccolithophores to climate change is likely to affect the marine carbon cycle in the future (Riebesell et al., 2017).

676

677

678

679 *Data availability.* The data are available upon request to the corresponding author
680 (yongzhang@fjnu.edu.cn).

681

682 *Author contributions.* YZ (yongzhang@fjnu.edu.cn), ZL and KX contributed to the
683 design of the experiment. YZ (yongzhang@fjnu.edu.cn), YZ
684 (qsx20211022@student.fjnu.edu.cn), SM, HC and RH performed this experiment and
685 biochemical analyses. YZ (yongzhang@fjnu.edu.cn) wrote the first manuscript draft.
686 All authors contributed to the data analyses and editing of the paper.

687

688 *Competing interests.* The authors declare that they have no conflict of interest.

689

690 *Acknowledgments.* We would like to thank Professor Zoe V. Finkel for providing the
691 *Emiliana huxleyi* RCC1266, Dr. Vinitha Ebenezer for her helpful revision of the
692 manuscript, and Dr. Peng Jin and two anonymous reviewers for their helpful
693 suggestions which have help us to improve the manuscript. This work was supported
694 by the National Natural Science Foundation of China (41806129 [YZ], 32001180
695 [ZKL]).

696

697

698

699

700

References

- Beaufort, L., Couapel, M., Buchet, N., Claustre, H., and Goyet, C.: Calcite production by coccolithophores in the southeast Pacific Ocean, *Biogeosciences*, 5, 1101–1117, doi:10.5194/bg-5-1101-2008, 2008.
- Berges, J. A., Franklin, D. J., and Harrison, P. J.: Evolution of an artificial seawater medium: improvements in enriched seawater, artificial water over the past two decades, *J. Phycol.*, 37, 1138–1145, doi: 10.1046/j.1529-8817.2001.01052.x, 2001.
- Borchard, C., Borges, A. V., Händel, N., and Engel, A.: Biogeochemical response of *Emiliania huxleyi* (PML B92/11) to elevated CO₂ and temperature under phosphorus limitation: A chemostat study, *J. Exp. Mar. Biol. Ecol.*, 410, 61–71, doi: 10.1016/j.jembe.2011.10.004, 2011.
- Caldeira, K., and Wickett, M. E.: Oceanography: anthropogenic carbon and ocean pH, *Nature*, 425, 365, doi: 10.1038/425365a, 2003.
- Chen, P., Toribara, T. T., and Warner, H.: Microdetermination of phosphorus, *Anal. Chem.*, 28, 1756–1758, doi: 10.1021/ac60068a036, 1956.
- Dickson, A. G., Sabine, C. L., and Christian, J. R.: Guide to best practice for ocean CO₂ measurements, *PICES Special Publication 3*, pp. 191, 2007.
- Dickson, A. G.: pH buffers for seawater media based on the total hydrogen ion concentration scale, *Deep-Sea Res.*, 40, 107–118, doi: 10.1016/0967-0637(93)90055-8, 1993.
- Dyhrman, S. T.: Nutrients and their acquisition: phosphorus physiology in microalgae, in: *The physiology of microalgae*, edited by: Borowitzka, M. A., Beardall, J. and Raven, J. A., Springer, Heidelberg, 155–183, doi: 10.1007/978-3-319-24945-2,

2016.

Fabry, V. J., and Balch, W. M.: Direct measurements of calcification rates in planktonic organisms, in: Guide to best practices for ocean acidification research and data reporting, edited by: Riebesell, U., Fabry, V. J., Hansson, L. and Gattuso, J. P., Luxembourg, Publications Office of the European Union, p. 201–212, doi: 10.2777/66906, 2010.

Feng, Y. Y., Roleda, M. Y., Armstrong, E., Summerfield, T. C., Law, C. S., Hurd, C. L., and Boyd, P. W.: Effects of multiple drivers of ocean global change on the physiology and functional gene expression of the coccolithophore *Emiliania huxleyi*, Glob. Chang. Biol., 26, 5630–5645, doi: 10.1111/GCB.15259, 2020.

Gao, K., Beardall, J., Häder, D. P., Hall-Spencer, J. M., Gao, G., and Hutchins, D. A.: Effects of ocean acidification on marine photosynthetic organisms under the concurrent influences of warming, UV radiation, and deoxygenation, Front. Mar. Sci., 6, 322, <https://doi.org/10.3389/fmars.2019.00322>, 2019.

Geider, R. J., and LaRoche, J.: Redfield revisited: variability of C:N:P in marine microalgae and its biochemical basis, Eur. J. Phycol., 37, 1–17, doi: 10.1017/S0967026201003456, 2002.

Gibbs, S. J., Poulton, A. J., Brown, P. R., Daniels, C. J., Hopkins, J., Young, J. R., Jones, H. L., Thiemann, G. J., O’Dea, S. A., and Newsam, C.: Species-specific growth response of coccolithophores to Palaeocene–Eocene environmental change, Nat. Geosci., 6, 218–222, doi: 10.1038/ngeo1719, 2013.

Guillard, R. R. L., and Ryther, J. H.: Studies of marine planktonic diatoms. I. *Cyclotella nana* Hustedt and *Detonula confervacea* Cleve, Can. J. Microbiol., 8, 229–239, doi: 10.1139/m62-029, 1962.

Hansen, H. P., and Koroleff, F.: Determination of nutrients, in: Methods of seawater

751 analysis, edited by: Grasshoff, K., Kremling, K. and Ehrhardt, M., WILEY-VCH
 752 Publishers, ISBN: 3-527-29589-5, 1999.

753 He, S., Le, C., He, J., and Liu, N.: Empirical algorithm for detecting coccolithophore
 754 blooms through satellite observation in the Barents Sea, *Remote Sens. Environ.*,
 755 270, 112886, doi: 10.1016/j.res.2021.112886, 2022.

756 Heidenreich, E., Wördenweber, R., Kirschhöfer, F., Nusser, M., Friedrich, F., Fahl, K.,
 757 Kruse, O., Rost, B., Franzreb, M., Brenner-Weiß, G., and Rokitta, S.: Ocean
 758 acidification has little effect on the biochemical composition of the
 759 coccolithophore *Emiliana huxleyi*, *PLoS One*, 14, e0218564, doi:
 760 10.1371/journal.pone.0218564, 2019.

761 Jin, P., Gao, G., Liu, X., Li, F., Tong, S., Ding, J., Zhong, Z., Liu, N., and Gao, K.:
 762 Contrasting photophysiological characteristics of phytoplankton assemblages in
 763 the Northern South China Sea, *PLoS ONE*, 11, e0153555, doi:
 764 10.1371/journal.pone.0153555, 2016.

765 Jin, P., Ding, J. C., Xing, T., Riebesell, U., and Gao, K. S.: High levels of solar
 766 radiation offset impacts of ocean acidification on calcifying and non-calcifying
 767 strains of *Emiliana huxleyi*, *Mar. Ecol. Prog. Ser.*, 568, 47–58, doi:
 768 10.3354/meps12042, 2017.

769 Jordan, R. W., and Winter, A: Assemblages of coccolithophorids and other living
 770 microplankton off the coast of Puerto Rico during January–May 1995, *Mar.*
 771 *Micropaleontol.*, 39, 113–130, doi: 10.1016/S0377-8398(00)00017-7, 2000.

772 Kondrik, D. V., Pozdnyakov, D. V., and Johannessen, O. M.: Satellite evidence that *E.*
 773 *huxleyi* phytoplankton blooms weaken marine carbon sinks, *Geophys. Res. Lett.*,
 774 45, e2017GL076240, doi: 10.1002/2017GL076240, 2018.

775 Kottmeier, D. M., Rokitta, S. D., and Rost, B.: Acidification, not carbonation, is the

major regulator of carbon fluxes in the coccolithophore *Emiliana huxleyi*, New
Phytol., 211, 126–137, doi: 10.1111/nph.13885, 2016.

Kubryakova, E. A., Kubryakov, A. A., and Mikaelyan, A. S.: Winter coccolithophore
blooms in the Black Sea: Interannual variability and driving factors, J. Mar. Syst.,
213, 103461, doi: 10.1016/j.jmarsys.2020.103461, 2021.

~~Larsen, A., Flaten, G. A. F., Sandaa, R., Castberg, T., Thyrrhaug, R., Erga, S. R.,
Jacquet, S., and Bratbak, G.: Spring phytoplankton bloom dynamics in
Norwegian coastal waters: Microbial community succession and diversity,
Limnol. Oceanogr., 49, 180–190, doi: 10.4319/lo.2004.49.1.0180, 2004.~~

Leonardos, K., and Geider, R. J.: Elevated atmospheric carbon dioxide increases
organic carbon fixation by *Emiliana huxleyi* (haptophyta), under nutrient-limited
high-light conditions, J. Phycol., 41, 1196–1203, doi:
10.1111/j.1529-8817.2005.00152.x, 2005.

Lohbeck, K., Riebesell, U., and Reusch, T. B. H.: Gene expression changes in the
coccolithophore *Emiliana huxleyi* after 500 generation of selection to ocean
acidification, Proc. R. Soc. B., 281, 20140003, doi: 10.1098/rspb.2014.0003,
2014.

Lu, Y., Wen, Z., Shi, D., Chen, M., Zhang, Y., Bonnet, S., Li, Y., Tian, J., and Kao, S.
J.: Effect of light on N₂ fixation and net nitrogen release of *Trichodesmium* in a
field study, Biogeosciences, 15, 1–12, doi: 10.5194/bg-15-1-2018, 2018.

Mackinder, L., Wheeler, G., Schroeder, D., von Dassow, P., Riebesell, U., and
Brownlee, C.: Expression of biomineralization-related ion transport genes in
Emiliana huxleyi, Env. Microbiol., 13, 3250–3565,
doi:10.1111/j.1462-2920.2011.02561.x, 2011.

Masuko, T., Minami, A., Iwasaki, N., Majima, T., Nishimura, S. I., and Lee, Y. C.:

801 Carbohydrate analysis by a phenol-sulfuric acid method in microplate format,
 802 Anal. Biochem., 339, 69–72, doi: 10.1016/j.ab.2004.12.001, 2005.

803 Matthiessen, B., Eggers, S. L., and Krug, S. A.: High nitrate to phosphorus regime
 804 attenuates negative effects of rising pCO₂ on total population carbon
 805 accumulation, Biogeosciences, 9, 1195–1203, doi: 10.5194/bg-9-1195-2012,
 806 2012.

807 McKew, B. A., Metodieva, G., Raines, C. A., Metodiev, M. V., and Geider, R. J.:
 808 Acclimation of *Emiliana huxleyi* (1516) to nutrient limitation involves precise
 809 modification of the proteome to scavenge alternative sources of N and P,
 810 Environ. Microbiol., 17, 4050–4062, doi: 10.1111/1462-2920.12957, 2015.

811 Meyer, J., and Riebesell, U.: Reviews and syntheses: responses of coccolithophores to
 812 ocean acidification: a meta-analysis, Biogeosciences, 12, 1671–1682, doi:
 813 10.5194/bg-12-1671-2015, 2015.

814 Moreno, A. R., and Martiny, A. C.: Ecological stoichiometry of ocean plankton, Ann.
 815 Rev. Mar. Sci., 10, 43–69, doi: 10.1146/annurev-marine-121916-063126, 2018.

816 Müller, M. N., Antia, A. N., and LaRoche, J.: Influence of cell cycle phase on
 817 calcification in the coccolithophore *Emiliana huxleyi*, Limnol. Oceanogr., 53,
 818 506–512, doi: 10.4319/lo.2008.53.2.0506, 2008.

819 Ni, G., Zimbalatti, G., Murphy, C. D., Barnett, A. B., Arsenault, C. M., Li, G.,
 820 Cockshutt, A. M., and Campbell, D. A.: Arctic *Micromonas* uses protein pools
 821 and non-photochemical quenching to cope with temperature restrictions on
 822 Photosystem II protein turnover, Photosynth. Res., 131, 203–220, doi:
 823 10.1007/s11120-016-0310-6, 2016.

824 Pakulski, J. D., and Benner, R.: An improved method for the hydrolysis and MBTH
825 analysis of dissolved and particulate carbohydrates in seawater, *Mar. Chem.*, 40,
826 143–160, doi: 10.1016/0304-4203(92)90020-B, 1992.

827 Perrin, L., Probert, I., Langer, G., and Aloisi, G.: Growth of the coccolithophore
828 *Emiliania huxleyi* in light- and nutrient-limited batch reactors: relevance for the
829 BIOSOPE deep ecological niche of coccolithophores, *Biogeosciences*, 13, 5983–
830 6001, doi: 10.5194/bg-13-5983-2016, 2016.

831 Pierrot, D., Lewis, E., and Wallace, D. W. R.: MS Excel program developed for CO₂
832 system calculations, ORNL/CDIAC-105, Carbon Dioxide Information Analysis
833 Centre, Oak Ridge National Laboratory, U.S., Department of Energy, doi:
834 10.3334/CDIAC/otg.CO2SYS_XLS_CDIAC105a, 2006.

835 R version 3.5.0.: The R foundation for statistical computing platform,
836 x86_64-w64-mingw32/x64. Available from:
837 <https://cran.r-project.org/bin/windows/base/old/3.5.0>, 2018.

838 Reith, M. E., and Cattolico, R. A.: Chloroplast protein synthesis in the chromophytic
839 alga *Olisthodiscus luteus*, *Plant Physiol.*, 79, 231–236, doi: 10.1104/pp.79.1.231,
840 1985.

841 Riebesell, U., Bach, L. T., Bellerby, R. G. J., Rafael Bermúdez Monsalve, J.,
842 Boxhammer, T., Czerny, J., Larsen, A., Ludwig, A., and Schulz, K. G.:
843 Competitive fitness of a predominant pelagic calcifier impaired by ocean
844 acidification, *Nat. Geosci.*, 10, 19–24, doi: 10.1038/NGEO2854, 2017.

845 Riegman, R., Stolte, W., Noordeloos, A. A. M., and Slezak, D.: Nutrient uptake and
846 alkaline phosphatase (EC 3:1:3:1) activity of *Emiliania huxleyi*
847 (Prymnesiophyceae) during growth under N and P limitation in continuous
848 cultures, *J. Phycol.*, 36, 87–96, 2000.

849 Rokitta, S. D., von Dassow, P., Rost, B., and John, U.: P- and N-depletion trigger
850 similar cellular responses to promote senescence in eukaryotic phytoplankton,
851 Front. Mar. Sci., 3, 109, doi: 10.3389/fmars.2016.00109, 2016

852 Rokitta, S. D., and Rost, B: Effects of CO₂ and their modulation by light in the
853 life-cycle stages of the coccolithophore *Emiliana huxleyi*, Limnol. Oceanog., 57,
854 607–618, doi: 10.4319/lo.2012.57.2.0607, 2012.

855 Rokitta, S. D., de Nooijer, L. J., Trimborn, S., de Vargas, C., Rost, B., and John, U.:
856 Transcriptome analyses reveal differential gene expression patterns between the
857 life-cycle stages of *Emiliana huxleyi* (haptophyta) and reflect specialization to
858 different ecological niches, J. Phycol., 47, 829–838, doi:
859 10.1016/S0924-9338(02)00624-7, 2011.

860 Rost, B., and Riebesell, U.: Coccolithophores and the biological pump: responses to
861 environmental changes, in: Coccolithophores : from molecular biology to global
862 impact, edited by: Thierstein, H. R. and Young, J. R., Springer, Berlin, 99–125,
863 2004.

864 Rouco, M., Branson, O., Lebrato, M., and Iglesias-Rodríguez, M.: The effect of
865 nitrate and phosphate availability on *Emiliana huxleyi* (NZEH) physiology
866 under different CO₂ scenarios, Front. Microbiol., 4, 1–11, doi:
867 10.3389/fmicb.2013.00155, 2013.

868 Roy, R. N., Roy, L. N., Vogel, K. M., Porter-Moore, C., Pearson, T., Good, C. E.,
869 Millero, F. J., and Campbell, D. C.: Thermodynamics of the dissociation of boric
870 acid in seawater at S 5 35 from 0 degrees C to 55 degrees C, Mar. Chem., 44,
871 243–248, doi: 10.1016/0304-4203(93)90206-4, 1993.

872 Shemi, A., Schatz, D., Fredricks, H. F., Van Mooy, B. A. S., Porat, Z., and Vardi, A.:
873 Phosphorus starvation induces membrane remodeling and recycling in *Emiliana*

874 *huxleyi*, New Phytol., 211, 886–898, doi: 10.1111/nph.13940, 2016.

875 Solórzano, L., and Sharp, J. H.: Determination of total dissolved phosphorus and
 876 particulate phosphorus in nature waters, Limnol. Oceanogr., 25, 754–758, doi:
 877 10.4319/lo.1980.25.4.0754, 1980.

878 Steinacher, M., Joos, F., Frölicher, T. L., Bopp, L., Cadule, P., Cocco, V., Doney, S.
 879 C., Gehlen, M., Lindsay, K., Moore, J. K., Schneider, B., and Segschneider, J.:
 880 Projected 21st century decrease in marine productivity: a multi-model analysis,
 881 Biogeosciences, 7, 979–1005, doi: 10.5194/bg-7-979-2010, 2010.

882 Sterner, R. W., and Elser, J. J.: Ecological Stoichiometry: The Biology of Elements
 883 from Molecules to the Biosphere, Princeton University Press, Princeton, 2002.

884 Terrats, L., Claustre, H., Cornec, M., Mangin, A., and Neukermans, G.: Detection of
 885 coccolithophore blooms with BioGeoChemical-Argo floats, Geophys. Res. Lett.,
 886 47, e2020GL090559, doi: 10.1029/2020GL090559, 2020.

887 Townsend, D. W., Keller, M. D., Holligan, P. M., Ackleson, S. G., and Balch, W. M.:
 888 Blooms of the coccolithophore *Emiliana huxleyi* with respect to hydrography in
 889 the Gulf of Maine, Cont. Shelf Res., 14, 979–1000, doi:
 890 10.1016/0278-4343(94)90060-4, 1994.

891 Tyrrell, T., and Merico, A.: *Emiliana huxleyi*: bloom observations and the conditions
 892 that induce them, in: Coccolithophores : from molecular biology to global impact,
 893 edited by: Thierstein, H. R. and Young, J. R., Springer, Berlin, 75–97, 2004.

894 Wang, C., Wang, J., Li, L., Wang, Y., and Lin, S.: P-limitation promotes carbon
 895 accumulation and sinking of *Emiliana huxleyi* through transcriptomic
 896 reprogramming, Front. Mar. Sci., 9, 860222, doi: 10.3389/fmars.2022.860222,
 897 2022.

898 Wang, G., Xie, S. P., Huang, R. X., and Chen, C.: Robust warming pattern of global

subtropical oceans and its mechanism, *J. Climate*, 28, 8574–8584, doi:
10.1175/jcli-d-14-00809.1, 2015.

Wilson, D. N., and Doudna Cate J. H.: The structure and function of the eukaryotic
ribosome, *CSH Perspect. Biol.*, 4, a011536, doi: 10.1101/cshperspect.a011536,
2012.

Zhang, Y., Collins, S., and Gao, K.: Reduced growth with increased quotas of
particulate organic and inorganic carbon in the coccolithophore *Emiliana*
huxleyi under future ocean climate change conditions, *Biogeosciences*, 17, 6357–
6375, doi: 10.5194/bg-17-6357-2020, 2020.

Zhang, Y., Li, Z. K., Schulz, K. G., Hu, Y., Irwin, A. J., and Finkel, Z. V.:
Growth-dependent changes in elemental stoichiometry and macromolecular
allocation in the coccolithophore *Emiliana huxleyi* under different
environmental conditions, *Limnol. Oceanogr.*, 66, 2999–3009, doi:
10.1002/lno.11854, 2021.

Figure Legends

Figure 1. Growth rate (**a**), cellular contents of particulate organic carbon (POC, **b**), nitrogen (PON, **c**) and phosphorus (POP, **d**), and particulate inorganic carbon (PIC, **e**) of *Emiliana huxleyi* RCC1266 in the treatments of high phosphorus availability and low CO₂ level (HP+LC), high phosphorus availability and high CO₂ level (HP+HC), low phosphorus availability and low CO₂ level (LP+LC), and low phosphorus availability and high CO₂ level (LP+HC) under low light (empty, 40 $\mu\text{mol photons m}^{-2} \text{ s}^{-1}$) and high light (fill, 300 $\mu\text{mol photons m}^{-2} \text{ s}^{-1}$) intensities. Different letters represent significant differences in each parameters between treatments ($p < 0.05$). The data represents the means and standard deviation of four independent cultures.

Figure 2. Cellular contents of carbohydrate (**a**) and protein (**b**), and the percentages of POC allocated to carbohydrate (**c**) and protein (**d**), and the percentage of PON allocated to protein (**e**) of *E. huxleyi* RCC1266 in the treatments of high phosphorus availability and low CO₂ level (HP+LC), high phosphorus availability and high CO₂ level (HP+HC), low phosphorus availability and low CO₂ level (LP+LC), and low phosphorus availability and high CO₂ level (LP+HC) under low light (empty) and high light (fill) intensities. Different letters represent significant differences in each parameters between treatments ($p < 0.05$). The data represents the means and standard deviation of four independent cultures. Please see figure 1 for more detailed information.

Figure 3. Cellular POC : POP ratio (**a**), PON : POP ratio (**b**), and protein content (**c**) of *E. huxleyi* RCC1266 as a function of growth rate, and cellular POC content as a

function of carbohydrate (**d**) in the treatments of high phosphorus availability and low CO₂ level (HP+LC, □), high phosphorus availability and high CO₂ level (HP+HC, ○), low phosphorus availability and low CO₂ level (LP+LC, △), and low phosphorus availability and high CO₂ level (LP+HC, ◇) under low light (LL, empty) and high light (HL, fill) intensities. Each point indicates an individual replicate under each treatment. Please see figure 1 for more detailed information.

Table 1. Carbonate chemistry parameters and dissolved inorganic phosphorus (DIP) concentration at the end of the incubation. The values are means \pm standard deviation (sd) of four replicates. Respectively, LL and HL represent 40 and 300 $\mu\text{mol photons m}^{-2} \text{ s}^{-1}$ of photosynthetically active radiation (PAR), and HP and LP represent 4 and 0.43 $\mu\text{mol L}^{-1} \text{ PO}_4^{3-}$ at the beginning of the incubations.

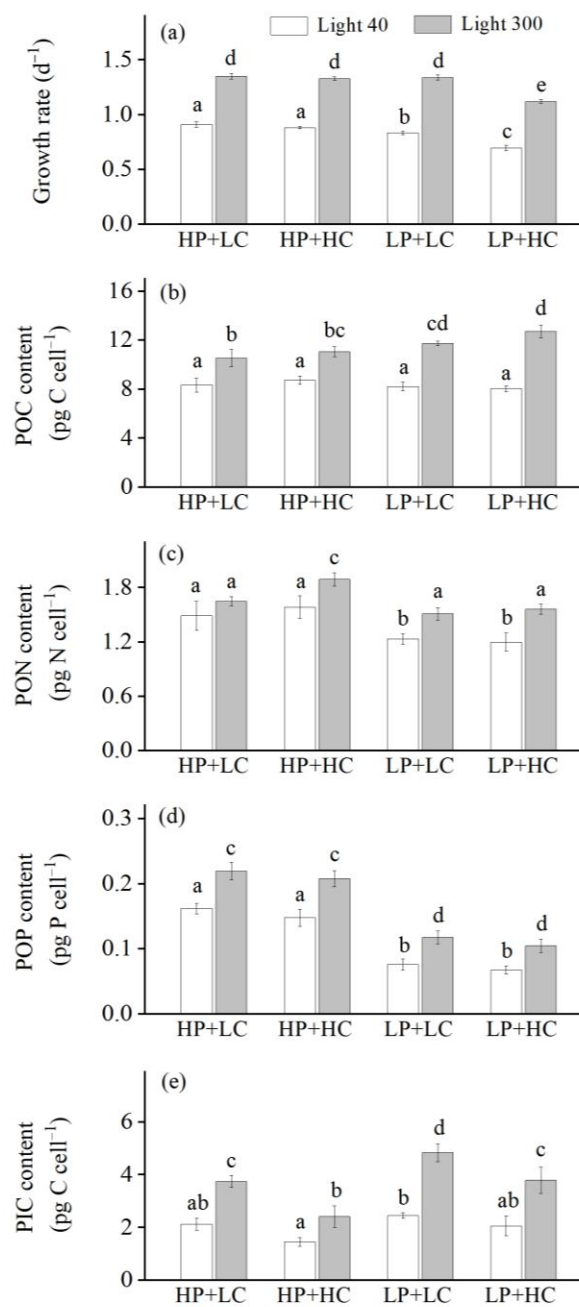
			$p\text{CO}_2$ (μatm)	pH (total scale)	TA ($\mu\text{mol L}^{-1}$)	DIC ($\mu\text{mol L}^{-1}$)	HCO_3^- ($\mu\text{mol L}^{-1}$)	CO_3^{2-} ($\mu\text{mol L}^{-1}$)	DIP ($\mu\text{mol L}^{-1}$)
LL	HP	LC	403 \pm 4	8.06 \pm 0.01	2346 \pm 23	2074 \pm 21	1861 \pm 18	200 \pm 2	3.20 \pm 0.03
		HC	881 \pm 20	7.77 \pm 0.01	2351 \pm 33	2216 \pm 32	2074 \pm 30	114 \pm 2	3.12 \pm 0.08
	LP	LC	329 \pm 4	8.13 \pm 0.01	2332 \pm 24	2024 \pm 22	1787 \pm 19	225 \pm 3	<0.04
		HC	730 \pm 8	7.84 \pm 0.01	2349 \pm 24	2189 \pm 23	2033 \pm 22	132 \pm 2	<0.04
HL	HP	LC	357 \pm 9	8.09 \pm 0.01	2235 \pm 41	1959 \pm 35	1749 \pm 30	199 \pm 6	2.86 \pm 0.06
		HC	791 \pm 7	7.80 \pm 0.01	2296 \pm 20	2151 \pm 20	2007 \pm 18	118 \pm 1	2.70 \pm 0.06
	LP	LC	303 \pm 4	8.16 \pm 0.01	2354 \pm 13	2024 \pm 11	1773 \pm 9	241 \pm 3	<0.04
		HC	735 \pm 19	7.83 \pm 0.01	2319 \pm 69	2162 \pm 65	2011 \pm 60	128 \pm 5	<0.04

Table 2. Growth rate (d^{-1}), cellular contents of POC, PON, POP, PIC, carbohydrate (CHO) and protein (Pro) ($pg\ cell^{-1}$), and the ratios of POC : PON, POC : POP, PON : POP and PIC : POC, and the percentages of POC allocated to carbohydrate (CHO-C : POC) and protein (Pro-C : POC), and the percentage of PON allocated to protein (Pro-N : PON) (%). LC and HC represent low CO_2 (426 μatm) and high CO_2 (946 μatm) levels, respectively. Please see table 1 for more detailed information.

	Low light intensity				High light intensity			
	HP		LP		HP		LP	
	LC	HC	LC	HC	LC	HC	LC	HC
Growth rate	0.91±0.03	0.88±0.01	0.83±0.02	0.70±0.03	1.35±0.03	1.33±0.02	1.34±0.02	1.12±0.02
POC	8.34±0.57	8.73±0.32	8.20±0.36	8.04±0.24	10.53±0.70	11.04±0.42	11.73±0.19	12.70±0.50
PON	1.49±0.16	1.58±0.12	1.23±0.06	1.20±0.10	1.65±0.05	1.89±0.07	1.51±0.07	1.56±0.06
POP	0.16±0.01	0.15±0.01	0.08±0.01	0.07±0.01	0.22±0.01	0.21±0.01	0.12±0.01	0.10±0.01
PIC	2.12±0.22	1.45±0.17	2.44±0.11	2.06±0.37	3.74±0.22	2.41±0.41	4.83±0.34	3.79±0.49
POC:PON	6.57±0.43	6.46±0.52	7.78±0.46	7.87±0.54	7.45±0.28	6.83±0.32	9.09±0.44	9.50±0.11
POC:POP	133.3±7.8	153.8±13.9	282.4±31.2	313.0±40.5	124.2±3.5	137.8±8.5	259.7±23.2	316.9±30.4
PON:POP	20.40±2.53	23.98±3.37	36.30±3.54	40.10±7.42	16.68±0.47	20.21±1.47	28.63±2.80	33.33±2.85
PIC:POC	0.26±0.04	0.17±0.02	0.30±0.02	0.26±0.04	0.36±0.02	0.22±0.04	0.41±0.03	0.30±0.04
CHO	1.45±0.15	1.81±0.16	1.79±0.16	1.94±0.16	3.58±0.41	4.30±0.17	4.96±0.24	5.85±0.49
Protein	5.23±0.55	5.37±0.39	3.73±0.27	3.80±0.15	6.45±0.36	6.97±0.22	6.25±0.29	6.28±0.30
CHO-C:POC	6.95±0.41	8.31±0.85	8.71±0.70	9.64±0.58	13.62±1.43	15.60±0.98	16.92±1.04	18.39±0.96
Pro-C:POC	33.26±3.24	32.58±1.98	24.15±2.52	25.07±1.69	32.49±1.69	33.51±1.41	28.23±1.35	26.21±1.27
Pro-N:PON	56.84±8.96	54.55±6.51	48.41±2.46	51.07±5.40	62.62±2.88	59.12±1.21	66.35±4.06	64.44±2.73

1009

1010



1011

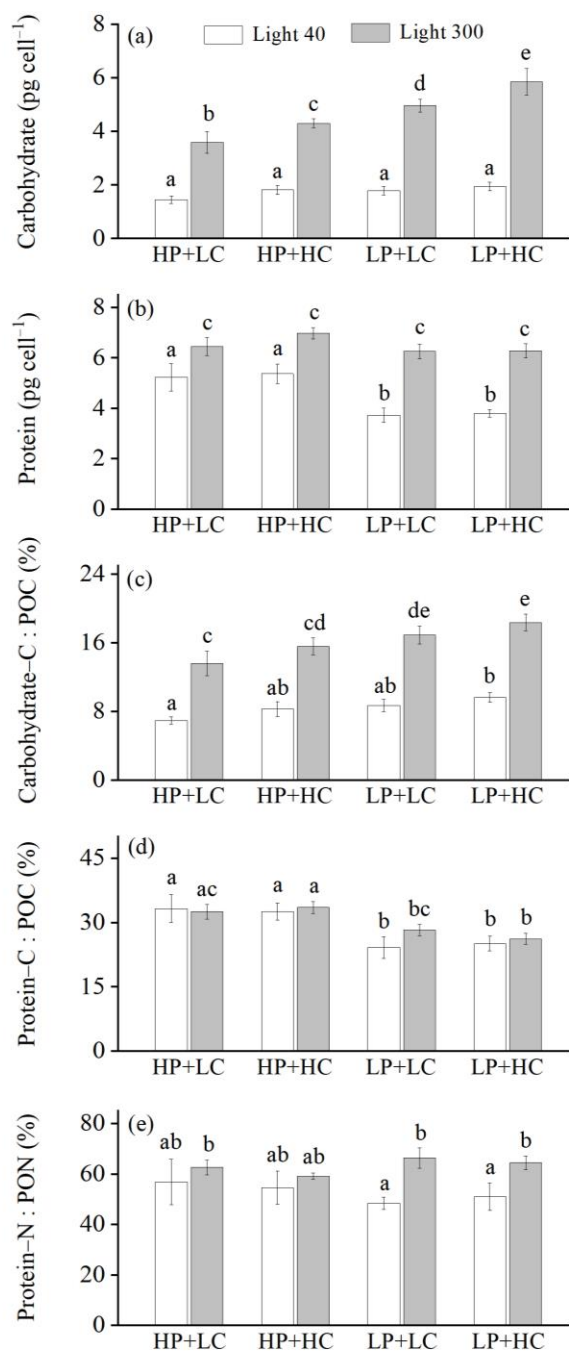
1012

1013 Figure 1

1014

1015

1016



1017

1018

1019 Figure 2

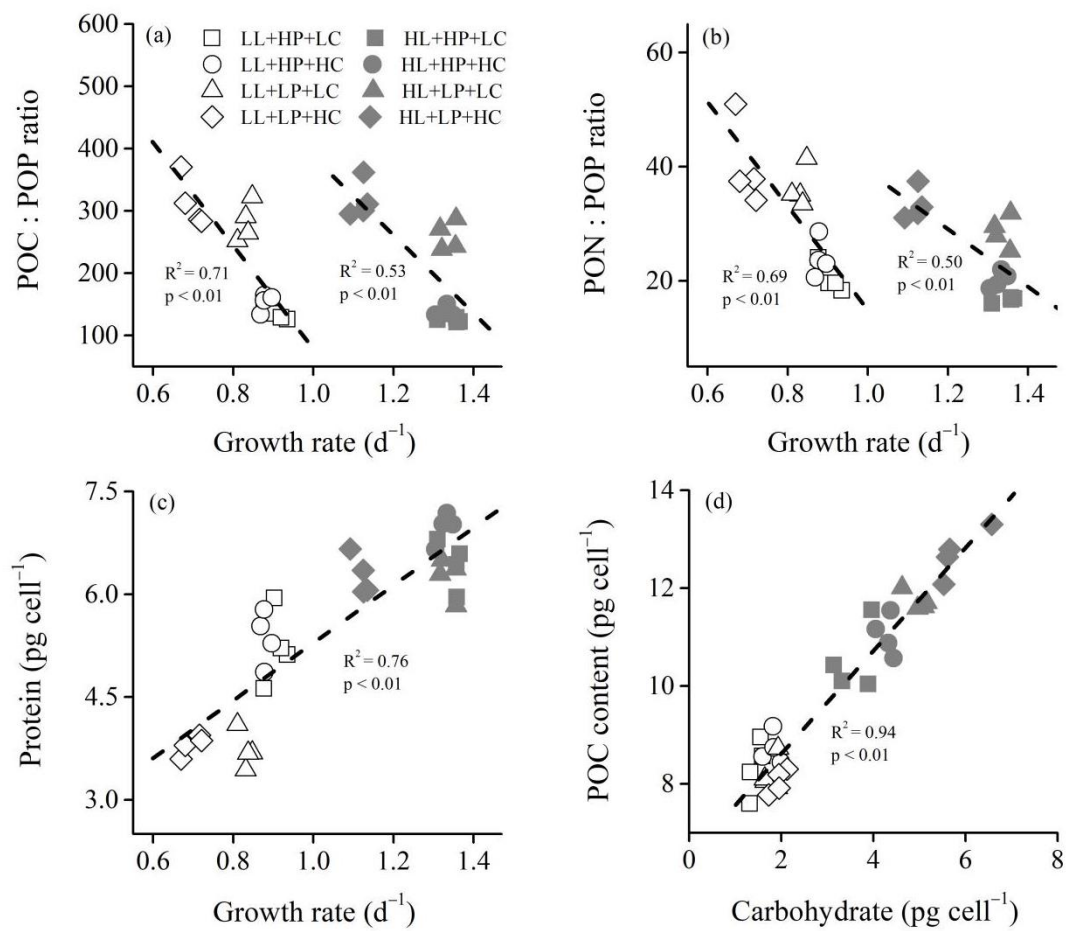


Figure 3